



Article

Alcohol triggers the accumulation of oxidatively-damaged proteins in neuronal cells and tissues.

Anusha W. Mudyanselage^{1,2}, Buddhika C. Wijamunige^{1,2}, Artur Kocoń¹, Ricky Turner¹, Denise McLean³, Benito Morentin⁴, Luis F. Callado⁵, and Wayne G. Carter^{1,*}

- ¹ Clinical Toxicology Research Group, School of Medicine, University of Nottingham, Royal Derby Hospital Centre, Uttoxeter Road, Derby, DE22 3DT, UK; artek.1993@googlemail.com (AK); ricky.turner@nhs.net (RT); Wayne.Carter@nottingham.ac.uk (WGC).
 - ² Department of Export Agriculture, Faculty of Agricultural Sciences, Sabaragamuwa University of Sri Lanka, Belihuloya 70140, Sri Lanka; wijesekara@agri.sab.ac.lk (AWM); buddhikawijamunige@agri.sab.ac.lk (BCW).
 - ³ School of Life Sciences, University of Nottingham, Nottingham, NG7 2UH. UK; denise.mclean@nottingham.ac.uk (DM).
 - ⁴ Section of Forensic Pathology, Basque Institute of Legal Medicine, Bilbao, Spain; morentin.b@justizia.eus (BM).
 - ⁵ Department of Pharmacology, University of the Basque Country, UPV/EHU, E-48940 Leioa, Bizkaia, and Centro de Investigación Biomédica en Red de Salud Mental, CIBERSAM, Spain; lf.callado@ehu.eus (LFC).
- * Correspondence: Wayne.Carter@nottingham.ac.uk (WGC); Tel.: (+44 (0)1332 724738)

Abstract: Alcohol is toxic to neurons and can trigger alcohol-related brain damage, neuronal loss, and cognitive decline. Neuronal cells may be vulnerable to alcohol toxicity and damage from oxidative stress after differentiation. To consider this further, the toxicity of alcohol to undifferentiated SH-SY5Y cells was compared with that of cells that had been acutely differentiated. Cells were exposed to alcohol over a concentration range of 0–200 mM for up to 24 hours and alcohol effects on cell viability were evaluated by MTT and LDH assays, and effects on mitochondrial morphology were examined by transmission electron microscopy and mitochondrial functionality by measurements of ATP and the production of reactive oxygen species (ROS). Alcohol reduced cell viability and depleted ATP levels in a concentration and exposure duration-dependent manner, with undifferentiated cells more vulnerable to toxicity. Alcohol exposures resulted in neurite retraction, altered mitochondrial morphology, and increased the levels of ROS in proportion to alcohol concentration and these peaked after 3- and 6-hour exposures and were significantly higher in differentiated cells. Protein carbonyl content (PCC) lagged ROS production and peaked after 12 and 24 hours, and increased in proportion to alcohol concentrations, with higher levels in differentiated cells. Carbonylated proteins were characterized by their denatured molecular weights and overlapped with those from adult post-mortem brain tissue, with levels of PCC higher in alcoholic subjects than matched controls. Hence, alcohol can potentially trigger cell and tissue damage from oxidative stress and the accumulation of oxidatively-damaged proteins.

Keywords: Alcohol; alcohol-related brain damage; developmental neurotoxicity; oxidative stress; protein carbonylation; reactive oxygen species.

Citation: To be added by editorial staff during production.

Academic Editor: Firstname Last-name

Received: date
Revised: date
Accepted: date
Published: date



Copyright: © 2024 by the authors. Submitted for possible open access publication under the terms and conditions of the Creative Commons Attribution (CC BY) license (<https://creativecommons.org/licenses/by/4.0/>).

1. Introduction

Ethyl-alcohol (ethanol) is the most widely imbibed, licit, psychoactive drug. Although drinking alcohol is an element of the social fabric of many cultures, there are serious health concerns and consequences that can arise from excessive alcohol intake [1–3]. The relationship between alcohol and human harm is complex and multidimensional but does increase monotonically with increased consumption [3]. The number of global deaths attributed to the harmful use of alcohol was over 3 million in 2016, constituting 1

in 20 deaths [4]. In terms of disability-adjusted life years (DALYs), over 5% of the global burden of disease is causally linked to alcohol usage [4,5].

The impact of alcohol on health relates to both the volume of alcohol consumed and the pattern of drinking, including the number of heavy drinking sessions [6]. Epidemiological analyses have established an association of alcohol usage with over 200 somatic diseases [7]. For some of these diseases, such as liver cirrhosis, a relative-risk dose-response exists [8] but the relationship between alcohol intake and risk of disease is not uniformly dose-dependent in all tissues. For some tissues, a curvilinear relationship such as a J or U-shaped curve may exist such that low to moderate drinkers have a reduced health risk than certain cohorts of abstainers. Although still a moot point, some epidemiological studies have suggested a protective benefit of low-level alcohol consumption for reduced risk of diabetes mellitus, ischemic heart disease, and dementia [7,9,10]. Nevertheless, the evidence base for long-term cognitive damage to alcoholics is probable. Some epidemiological studies have suggested a reduced risk of development of dementia for certain minimal and light drinking cohorts when compared to abstainers, but many studies have concluded that heavy drinking is associated with an increased risk of dementia and cognitive decline [11-17].

In support of an association between excessive alcohol drinking and dementia; brain atrophy, damage, and neuronal loss have all been detected in many but not all post-mortem studies of the brains of alcoholics [18-25]. Likewise, brain shrinkage of white and/or grey matter in response to longitudinal alcohol exposure has been detected using a range of in vivo imaging techniques [26-34]. Furthermore, specific localised volumetric reductions of subcortical structures including the prefrontal cortex and hippocampal regions have also been detected in alcoholics [30,32], and correlate with cognitive decline [32].

Adolescence is a period of notable vulnerability to the neurotoxic effects of alcohol, with binge drinking associated with reduced grey matter and detrimental effects on attention and cognition [35, 36]. The elderly may also be more responsive to the toxic effects of alcohol [36], and there is a decline in brain structure with age that mirrors that observed in alcoholic patients [25]. Alcohol also has teratogenic effects, such that excessive maternal alcohol consumption during pregnancy impacts the neurodevelopment of the foetus and results in foetal alcohol spectrum disorders (FASD), and negative effects on cognition [36-40]. FASD is recognized by the presence of a range of impairments to growth, dysmorphia, and central nervous system (CNS) dysfunction, including deficits in cognition and neurobehavioural abnormalities as a consequence of brain damage [36-40]. Reduced grey and white matter contribute to the collective reduction in brain size for babies with FASD [39,40]. Alcohol may therefore be particularly neurotoxic during periods of neurodevelopment and in the elderly, and this could be mediated by mechanisms including cellular redox stress and induction of apoptosis [40-43].

Excessive alcohol exposure can result in a depletion of neuronal number (cell death) but alcohol also has a broad impact on neurocircuitry and plasticity [40,44] and these could diminish the functionality of surviving neurons [39,40,45]. Hence, to gain more insight into the effects of alcohol on newly differentiated neuronal cells, and the potential impact of oxidative stress, the toxicity of alcohol was directly compared between undifferentiated and differentiated SH-SY5Y cells. Neurotoxicity was assessed via quantitation of alcohol effects on cell viability, mitochondrial morphology and functionality, the induction of reactive oxygen species (ROS), and the accumulation of oxidatively-damaged proteins. Studies were also undertaken to consider if the oxidative damage observed in cells after alcohol exposure was mirrored by that present within human post-mortem brain tissue from alcoholics.

2. Materials and Methods

2.1 Cell culture and cell image capture

The SH-SY5Y human neuroblastoma cell line was purchased from the European Collection of Authenticated Cell Culture (ECACC) (ECACC-94030304). Experiments were

conducted with cells from passages 13–14. SH-SY5Y cells were grown in the following culture medium: 43.5% Eagle's Minimum Essential Medium (EMEM) (M4655, Sigma, Poole, UK) supplemented with 43.5% Ham's F12 nut mix (217665-029, Gibco, Waltham, USA), 10% heat-inactivated Fetal Bovine Serum (FBS) (F9665, Sigma, Poole, UK), 1% MEM Non-Essential Amino Acid Solution (NEAA) (RNBF3937, Sigma, Poole, UK), 2 mM glutamine, and 1% penicillin–streptomycin solution containing 10,000 IU penicillium and 10 mg/mL streptomycin (p/s) (P4333, Sigma, Poole, UK) in 25 or 75 cm² flasks (ThermoFisher scientific, Rochester, UK) at 37°C with an atmosphere of 5% CO₂ and 95% humidity, as previously described [46]. Cells were observed daily and grown until the cells reached approximately 80% confluence, after which the culture medium was refreshed every other day.

For differentiation, SH-SY5Y cells were seeded on either poly-D-Lysine (PDL) hydrobromide (5 mg/mL) (P6407, Sigma, Poole, UK) coated 25 cm² flasks (T25, 130189, ThermoFisher Scientific, Rochester, UK) or in 96 well microtiter plates (6005649, Perkin Elmer, Groningen, Netherlands) with 10% FBS media. After the cells had settled, they were grown to 60% confluency. The following day, the cells were treated with differentiation media (10 µM all-trans retinoic acid (RA) (R2625, Sigma, Poole, UK) in low serum SH-SY5Y medium (1% FBS) for 6 days, and then treated with 20 ng/mL brain-derived neurotrophic factor (BDNF) (B3795, Sigma, Poole, UK) with low serum media containing RA for 2 more days, after which the cells displayed a fully differentiated morphology [46,47].

Cells treated with alcohol (10–200 mM) were monitored with an inverted microscope with phase contrast optics (Olympus, DP70, London, UK) to compare the general morphological changes with untreated controls for both undifferentiated and differentiated cells at the end of the treatment period. Cells that were cultured in 12-well PDL-coated plates were used to study the neurite length changes in differentiated cells in response to 0–200 mM alcohol treatments. Cells were considered to be differentiated if each neuronal cell contained at least one process that was longer than its cell body [48]. The neurite length from 200 randomly chosen cells was measured in 5 selected quadrants per well using the neurite tracer tool from Image J (Image J 1.49k, National Institute of Health, USA) in three independent wells for one treatment [49].

Untreated cells or those incubated with alcohol for 24 hours were prepared for transmission electron microscopy (TEM) according to the methods described in [50]. In brief, after a 24 hour incubation, the medium was removed and cells were washed with medium containing fixative (3% glutaraldehyde in 0.1 M cacodylate buffer). The media:fixative solution (1:1 (v/v)) was then replaced with fixative alone before the cells were fixed in an incubator for 1 hour at 37°C. Cells were scraped into the fixative, collected by centrifugation, and then further fixed at 4°C for 1 hour. Cells were then washed in a 0.1M cacodylate buffer, and transferred to flat-bed embedding capsules, before an incubation with 1% osmium tetroxide in 0.1 M cacodylate buffer for 1 hour. Cells were water-washed and then dehydrated using a series of ethanol solutions: 50, 70, 90 and 100% ethanol, and a transitional solution, 100% propylene oxide. Cells were then infiltrated with an epoxy resin:propylene oxide mix (1:1) overnight. The following day, the samples were infiltrated with epoxy resin for 3 x 2 hours and then embedded and polymerized by heating at 60°C for 48 hours. Ultra-thins (80 nm) of the cells were sectioned with a diamond knife on a Leica EM UC6 ultramicrotome, mounted on 200 mesh copper grids, and then analysed using a Tecnai G2 BioTWIN TEM (FEI company, Eindhoven, The Netherlands).

2.2 Thiazolyl Blue Tetrazolium Bromide (MTT) assays

Cell metabolic activity and cell viability were determined using a Thiazolyl Blue Tetrazolium Bromide (MTT) (M5655, Sigma, Poole, UK) assay as described previously [51]. SHSY-5Y cells were seeded at 3 x 10⁴ cells/well in 96 well plates with growth media (10% FBS). After 24 hours, undifferentiated cells were exposed to ethanol (0–200 mM) diluted in growth media (10% FBS). Differentiated cells were prepared as described above and then treated with ethanol (0–200 mM) diluted in differentiation media supplemented with 20 ng/mL BDNF. After incubation, spent media was removed, and then replaced with

media containing 10% 5 mg/mL MTT, and incubated for 4 hours. Plate wells which only received 10% MTT and respective growth media served as background controls. The generated formazan crystals were suspended in a 1:1 dimethyl sulphoxide (DMSO, D8418, Sigma, Poole, UK): isopropanol (279544, Sigma, Poole, UK) solution. The absorbance of wells was then read at 570 nm using a spectrophotometer (Multiskan Spectrum, Thermo Electron Corporation, Finland). An average value was calculated from experiments performed in triplicates after the subtraction of blank (negative control) values. Cell viability was expressed as a percentage of survival compared to that from mock-treated cells. The inhibitor concentrations producing a 50% loss of viability of cells (IC₅₀ values) were obtained from the concentration-response curves and expressed as means ± standard deviation (SD).

2.3 Lactate dehydrogenase (LDH) assays

Undifferentiated or differentiated SHSY-5Y cells were prepared as described above for the MTT assay and similarly treated with ethanol. After ethanol treatment, 50 µL of spent media was removed and LDH activity determined using an assay kit (ab102526, Abcam, Cambridge, UK) according to the manufacturer's guidelines. NADH standards were prepared according to the manufacturer's protocol and were transferred into the same assay plate. Assays were performed at 450 nm using a spectrophotometer (Multiskan Spectrum, Thermo Electron Corporation, Finland) in kinetic mode, with readings every 2 minutes at 37°C, protected from light, for a total of 60 minutes. A NADH standard curve was generated and LDH activity measurements interpolated from the NADH standard curve. An average value was calculated from experiments performed in triplicates after the subtraction of blank (negative control) values.

2.4 Adenosine 5'-triphosphate (ATP) assays

Undifferentiated SH-SY5Y cells were seeded in 6 well plates (CC7682-7506, STARLAB International GmbH, Hamburg, Germany) at a density of 1×10⁶ cells/well for analysis. For differentiated cells, cells were seeded at 5 × 10⁴ cells/well in PDL-coated 6 well plates, with the differentiation protocol followed for 7 days as described above. Cells were treated with ethanol as before, and ATP levels were quantified using an ATP luminescence assay kit (ATP Bioluminescence Assay Kit CLS II (11 699 695 001, Roche, Germany), as per the manufacturer's protocol. The ATP content in control and ethanol-treated samples was interpolated from an ATP standard curve as described previously [52]. An average value was calculated from experiments performed in triplicates after the subtraction of blank (negative control) values.

2.5 Measurements of reactive oxygen species

The generation of reactive oxygen species (ROS) was quantified using a 2',7'-dichlorofluorescein diacetate (DCFDA) (D6883, Sigma, Poole, UK) assay. SHSY-5Y cells were seeded at 3 × 10⁴ cells/well in clear bottom black 96 well plates (165305, ThermoFisher Scientific, Rochester, UK) with growth media (at 10% FBS). After 24 hours, undifferentiated cells were exposed to ethanol (0–200 mM) diluted in growth media (10% FBS) and differentiated cells were prepared as described above and then treated with ethanol (0–200 mM) diluted in differentiation media supplemented with 20 ng/mL BDNF and 10 µM RA. Cells were treated with ethanol for 3, 6, 12, or 24 hours, with 50 µM DCFDA included for the experiment duration. Cells were washed twice with ice-cold PBS and then fluorescence quantified using a Varioskan™ LUX multimode microplate reader (ThermoFisher Scientific, Waltham, MA, USA) at excitation and emission spectra of 495 nm and 529 nm, respectively. Hydrogen peroxide (0.5 mM) was used as a positive control for ROS and set as 100% fluorescence [46,53]. Three to six replicate assays were performed for all data points, from which an average was calculated.

2.5 Cell lysis

After ethanol or vehicle treatment of undifferentiated or differentiated SH-SY5Y cells, cells were washed with cold phosphate buffered saline (PBS) (10010015, Life Technologies, Paisley, UK) before addition of 0.5 mL of radioimmunoprecipitation assay (RIPA, 20-188, Millipore, USA) buffer containing protease inhibitors (04693124001, mini-

protease inhibitor cocktail, Sigma, Poole, UK) and a phosphatase inhibitor cocktail (P0044, Sigma, Poole, UK) and flask agitation on ice for 5 minutes. Cells were then scraped into the RIPA buffer, vortexed thoroughly, and then homogenized by passage through a 28g needle 25 times. Homogenates were stored at -20°C until required.

2.6 Protein quantification

The quantitation of protein concentration was performed based on the Lowry assay [54]. Bovine serum albumin (BSA) protein was used as a protein standard. The modified Lowry assay was performed in 96 well plates using protein standard amounts of 1.25, 2.5, 5, 7.5, and 10 µg of protein. For a volume of 40 µL of cell lysates or protein standards, 20 µL of Reagent A was added and then 160 µL of Reagent B. After 15 minutes, spectrophotometric measurements were taken at 740 nm using a Spectramax plate reader (Multiskan Spectrum, Thermo Electron Corporation, Finland). Protein amounts of unknowns were interpolated from the BSA standard curve.

2.7 Determination of protein carbonyl content

Undifferentiated or differentiated SH-SY5Y cells were grown to 80% confluence and then treated with ethanol for 3, 6, 12, or 24 hours, as described above. After alcohol treatment, cells were washed with ice cold PBS three times and then solubilized and lysed with RIPA buffer containing protease and phosphatase inhibitors (according to Section 2.5). Samples were vortexed for 30 seconds and then sonicated for 15 minutes on ice-cold water. Samples were then spun at 500 x g for 10 minutes at 4°C, and the supernatant was retained and centrifuged at 23,100 x g for 40 minutes at 4°C to prepare a crude cytosolic fraction [24]. Protein concentration was determined using a modified Lowry assay (according to Section 2.6) and then adjusted to 1 mg/mL for cells or brain tissue homogenates (refer to Section 2.9). An equivalent volume of 10 mM 2,4-dinitrophenylhydrazine (DNPH) (Sigma-Aldrich, Poole, UK) prepared in 2N HCL (231-5957, Scientific Laboratory Suppliers, Nottingham, UK) was added to samples or blanks, vortex mixed, and then samples left in the dark for 1 hour at room temperature, with vortex mixing every 10 minutes. Protein precipitation was initiated by the addition of an equivalent volume of ice-cold 20% (w/v) trichloroacetic acid (TCA) (Sigma-Aldrich, Poole, UK) and then samples were retained on ice for 15 minutes. The precipitate was washed according to previously published methods [46], before solubilization in 6 M guanidine hydrochloride (50950, Fluka Chemie AG, Buchs, Switzerland) in 50 mM phosphate buffer, pH 2.3, with incubation at 37°C for 30 mins and with vortex mixing. The protein carbonyl content (PCC) was then determined spectrophotometrically (Thermo Fisher Scientific, Fluoroskan Ascent FC, Finland) at 366 nm using a molar absorption coefficient of 22,000 M⁻¹cm⁻¹ after subtraction of blanks. Data points were generated from assays performed in triplicate from which an average was calculated.

2.8 Western oxy-blotting

Immuno-blotting for reactive carbonyl groups (oxidatively-damaged proteins) was undertaken using an OxyBlot Protein Oxidation Detection Kit (S7150, Millipore, USA) as recommended by the manufacturer. Cytosolic protein concentrations were quantified as detailed above using a modified Lowry assay (Section 2.6). Proteins were then prepared to a concentration of 2 mg/mL via the addition of 12% sodium dodecyl sulphate (SDS) and 2,4-dinitrophenylhydrazine (DNPH) solution, and carbonyl groups derivatized by incubation at room temperature for 15 minutes. Neutralization solution and then β-mercaptoethanol were added to the sample mixture, and then proteins resolved using Novex NuPAGE 10% Bis-Tris gels (ThermoFisher scientific, Rochester, UK) run in an Xcell sure-lock mini-cell system with (3-N-morpholino)propanesulphonic acid (MOPS) running buffer (ThermoFisher scientific, Rochester, UK) as described previously [55]. Gel proteins were transferred in a BioRad mini trans-blot cell to polyvinylene difluoride (PVDF) (Millipore, USA) membranes and probed with a rabbit anti-DNP primary antibody, followed by a goat anti-rabbit IgG (horseradish peroxidase (HRP)-conjugated) secondary antibody as described previously [46]. Immunoreactivity was detected using a ChemiDoc MP

imager (BioRad, Hertfordshire, UK), with light captured with an autoexposure setting to ensure signal linearity.

2.9 Human brain samples

The human brain samples used in this study were used in accordance with the Human Tissue Act (2004) (UK) and were supplied by the Neuropsychopharmacology Research Group from the Department of Pharmacology of the University of the Basque Country (UPV/EHU). (<https://www.ehu.es/en/web/neuropsicofarmacologia/home>). Brain collection was conducted in compliance with policies of research and ethical review boards for post-mortem brain studies (Basque Institute of Legal Medicine, Bilbao, Spain) and is registered in the National Biobank Register of the Spanish Health Department with the study number C.0000035 (<https://biobancos.isciii.es/ListadoColecciones.aspx>). The diagnosis of alcoholism was carried out according to the Diagnostic and Statistical Manual of Mental Disorders (DSM-III-R, DSM-IV or DSM-IV-TR; American Psychiatric Association) or International Classification of Diseases criteria (ICD-10; World Health Organization). All diagnoses were established by clinicians in charge of the patients prior to death. Six control brain samples were used, matched by age and sex, to 6 alcoholic subjects, as detailed in previous studies [24,25, Supplementary Table S1]. Toxicological screening of the blood (quantitative assays for antidepressants, antipsychotics, other psychotropic drugs, and ethanol) was performed at the National Institute of Toxicology, Madrid, Spain. The brain samples used were all from the prefrontal cortex (Brodmann's area 9) (BA 9), macroscopically dissected at the time of autopsy, and stored at -80°C until required.

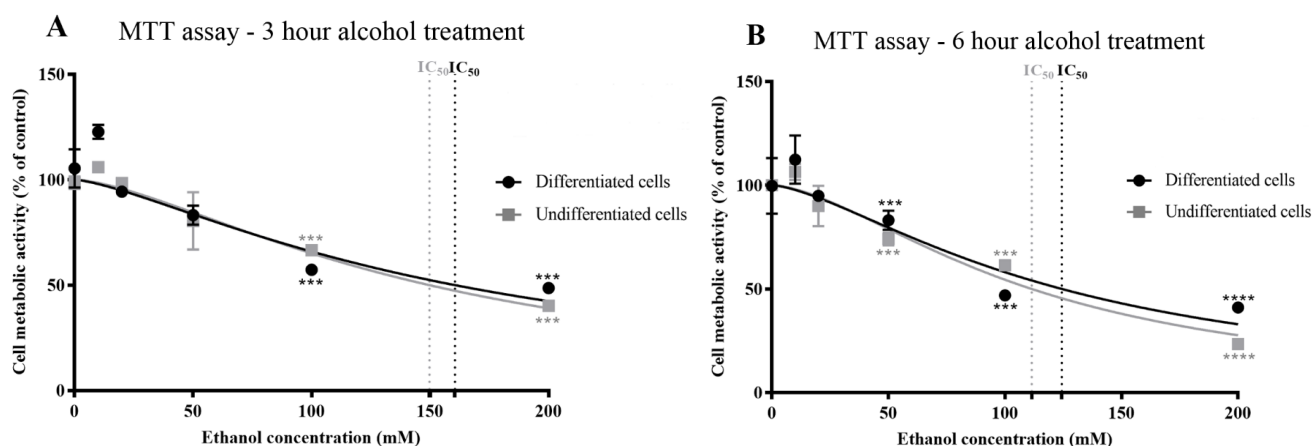
2.11 Statistical analysis

Data for cell viability and ATP assays are presented as means \pm standard error of the mean (SEM). Statistical analysis was performed using GraphPad Prism 9.2.0 (GraphPad Prism, San Diego, CA, USA). Concentration-response curves were plotted using a non-linear regression curve fit model as lines of best fit. To assess differences between control and treatment groups, a one-way analysis of variance (ANOVA) or two-way ANOVA with Dennett's multiple comparison test and Tukey's multiple comparisons, respectively, were performed. Results were considered significant at a p-value below 0.05.

3. Results

3.1 Alcohol effects on cell viability

Undifferentiated and differentiated SH-SY5Y cells were exposed to alcohol at concentrations of 0–200 mM for 3, 6, 12, or 24 hours and cell metabolic activity and viability were quantified using an MTT assay (Figures 1A–D). Alcohol reduced cell metabolic activity and viability in a concentration and exposure duration-dependent manner from a threshold of ≥ 20 mM for either undifferentiated or differentiated SH-SY5Y cells (Figure 1A–D and Supplementary Table S2).



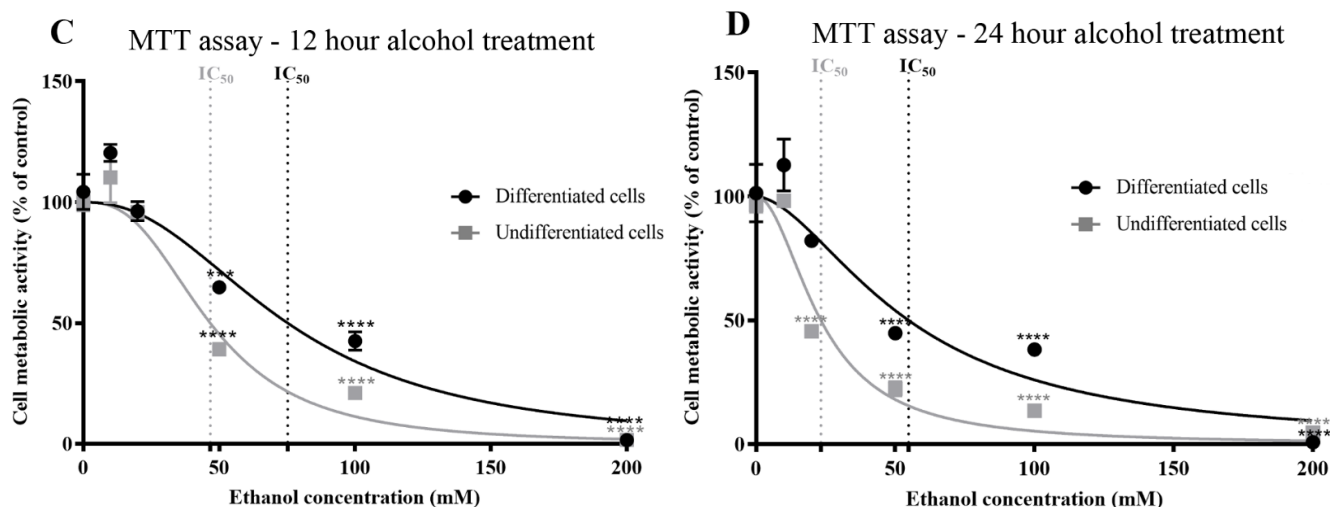


Figure 1: Alcohol effects on cellular metabolic activity and viability determined using an MTT assay.

Undifferentiated or differentiated SH-SY5Y cells were exposed to alcohol (0–200 mM) for durations of 3 (A), 6 (B), 12 (C), and 24 (D) hours and the levels of metabolic activity and cell viability quantified using an MTT assay. Each data point represents a mean of at least 5 individual experiments. For marked significance: *** = p -value < 0.001, **** = p -value < 0.0001.

After a 3 or 6-hour alcohol exposure, cell metabolic activity for both undifferentiated or differentiated SH-SY5Y cells was similar and inversely proportional to alcohol concentration, such that there was an approximately linear decline in cell viability with increasing alcohol concentration (Figures 1A,B). After a 12 or 24-hour incubation with alcohol, the inhibitor-response curves showed a significant reduction of cell viability at 50 mM alcohol ($p < 0.0001$) (Figures 1C,D). Differentiated cells were more resistant to alcohol toxicity than undifferentiated cells, with higher concentrations required to induce a 50% inhibition of cell viability (IC_{50}) (Figures 1A–D, Table 1, and Supplementary Table S3). The lowest concentration of alcohol examined (10 mM) increased cell metabolic activity, although non-significantly ($p = 0.113$), by 6–11% in differentiated cells and 1–10% in undifferentiated cells ($p = 0.08$) (Figures 1A–D).

Table 1: Toxicity of alcohol to undifferentiated and differentiated SHSY-5Y cells.

Cell Type	Treatment duration (hours)	MTT assay		LDH assay		ATP assay	
		IC ₅₀	R ²	IC ₅₀	R ²	IC ₅₀	R ²
Undifferentiated	3	149.8 ± 18.6	0.8800	110.6 ± 3.1	0.9878	158.5 ± 17.3	0.9149
Differentiated		160.5 ± 25.8	0.7969	172.5 ± 3.4	0.9863	179.4 ± 26.3	0.7732
Undifferentiated	6	111.5 ± 7.6	0.9453	107.2 ± 4.6	0.9722	124.4 ± 10.6	0.9430
Differentiated		124.4 ± 14.7	0.8573	136.1 ± 5.9	0.9507	158.2 ± 29.2	0.7196
Undifferentiated	12	46.7 ± 3.1	0.9648	46.9 ± 3.1	0.9743	42.2 ± 3.9	0.9445
Differentiated		75.25 ± 7.0	0.9268	75.8 ± 4.5	0.9551	74.4 ± 3.7	0.9745
Undifferentiated	24	23.3 ± 2.1	0.9372	24.9 ± 2.374	0.9371	36.0 ± 5.1	0.8476
Differentiated		54.83 ± 6.5	0.9016	59.10 ± 2.3	0.9391	48.08 ± 3.4	0.9551

Since MTT assays provide insight into cell metabolic activity and this may not always correlate with cell viability, the liberation of extracellular LDH was used as an independent method for the determination of cell viability in response to alcohol. Similar to the MTT assays, undifferentiated and differentiated cell viability decreased in proportion to the alcohol concentration and length of exposure time (Figures 2A-D and Supplementary Table S4). The threshold for a significant reduction of cell viability was a concentration of alcohol of ≥ 20 mM for a 6-hour exposure time ($p < 0.001$ for undifferentiated cells and p

< 0.0001 for differentiated cells) (Figure 2B). Non-linear regression analysis showed that undifferentiated cells were more sensitive to the toxic effects of alcohol, with lower IC₅₀ concentrations, in keeping with the MTT data (Table 1 and Supplementary Table S2).

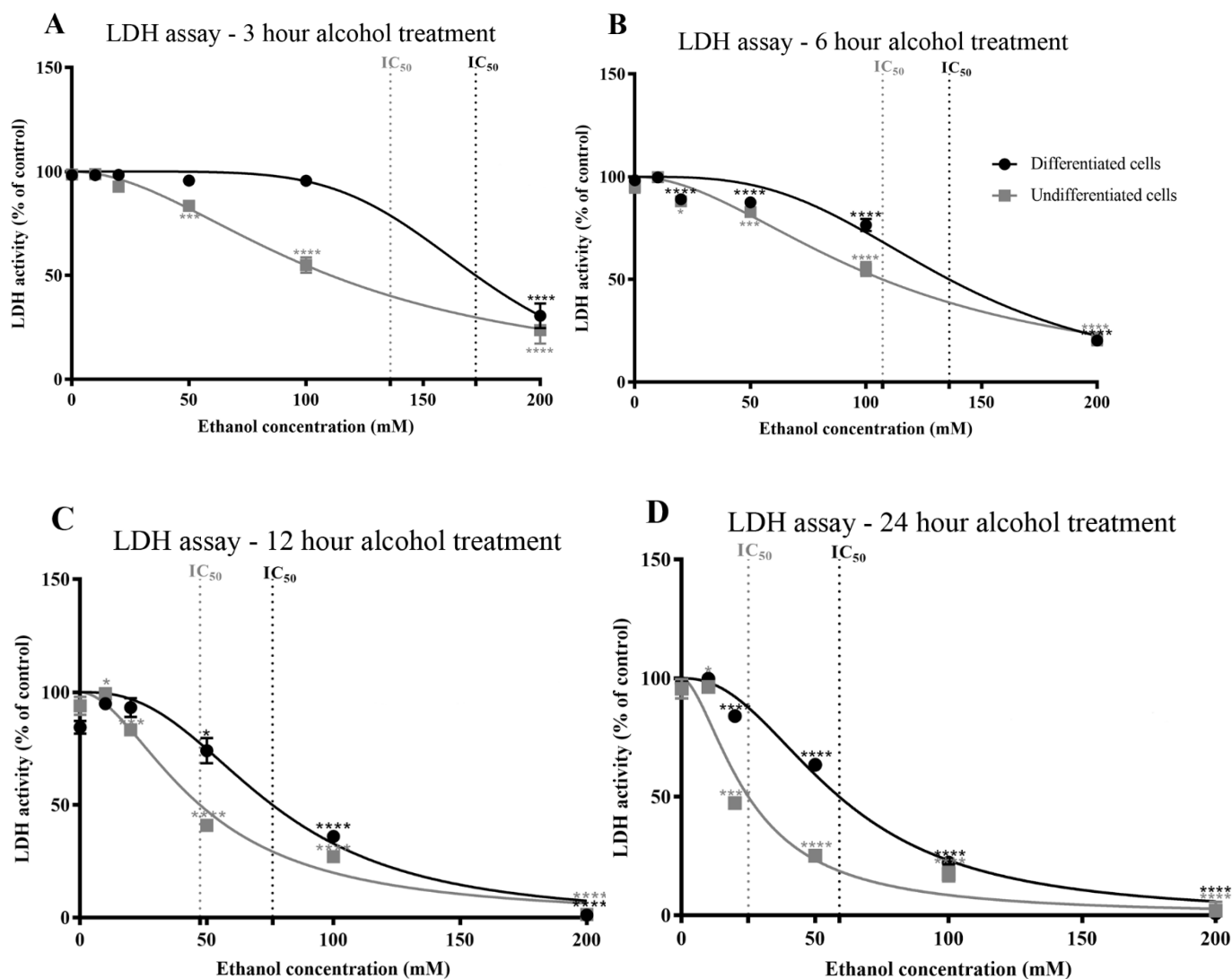


Figure 2: Alcohol effects on cell viability determined using an LDH activity assay. Undifferentiated or differentiated SH-SY5Y cells were exposed to alcohol (0–200 mM) for durations of 3 (A), 6 (B), 12 (C), and 24 (D) hours, and the activity of extracellular LDH was quantified. Each data point represents the mean of at least 5 individual experiments. For marked significance: * = p-value < 0.05, *** = p-value < 0.001, **** = p-value < 0.0001

Additionally, the alcohol-induced reduction in cell viability and influence on neuritic projections (Figure 3) were assessed by direct observation of the cells and photographic image capture (Supplementary Figure S1) and Supplementary Table S5). Alcohol triggered a significant reduction in neuritic arborization from a threshold concentration of 50 mM for 6 ($p < 0.001$), 12 ($p < 0.001$), and 24-hour ($p < 0.001$) exposures (Figure 3).

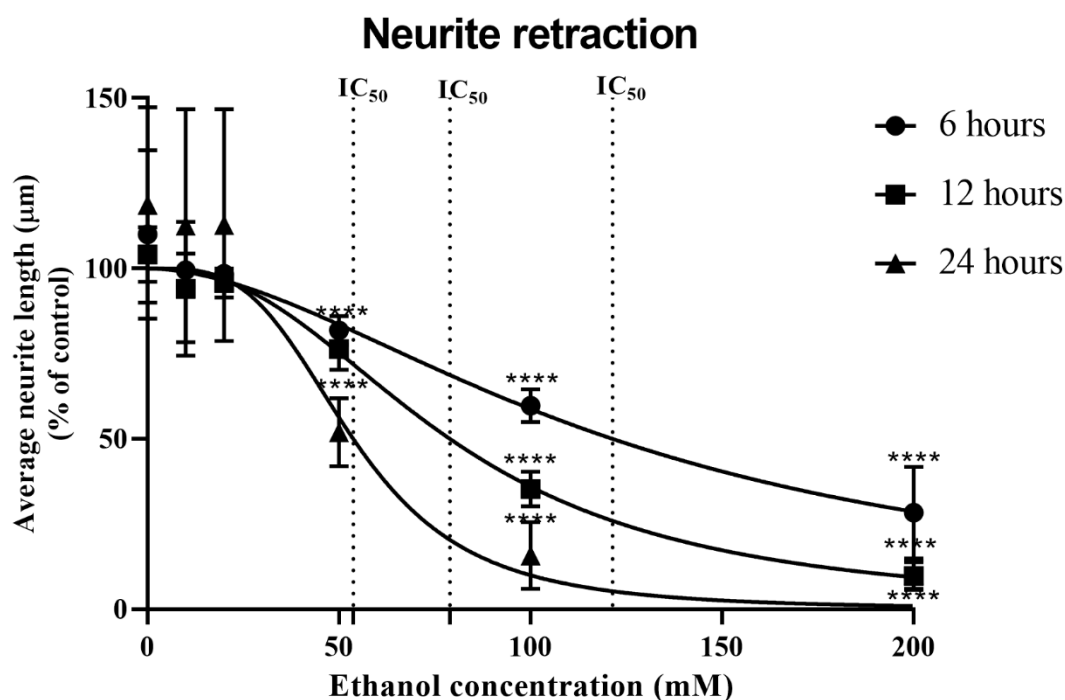


Figure 3: Neurite retraction in response to alcohol treatment.

Differentiated SHSY-5Y cells were treated with alcohol over a concentration range of 0–200 mM for 6–24 hours and the length of neuritic projections was quantified. Experiments were conducted in triplicate and each data point represents the mean of at least 5 individual experiments (\pm SD), with vehicle control experiments set at 100%. Significant reductions of neuritic projections were observed at 50 mM alcohol and for all time points. For marked significance: **** = p-value < 0.0001.

3.1 Alcohol effects on cellular bioenergetics and the liberation of reactive oxygen species

Direct effects on mitochondrial morphology were examined using transmission electron microscopy (TEM) (Figures 4A-D). Alcohol at concentrations of ≥ 50 mM increased the opacity of mitochondria (less electron dense) and some vacuoles were present within cells, that may reflect mitophagy.

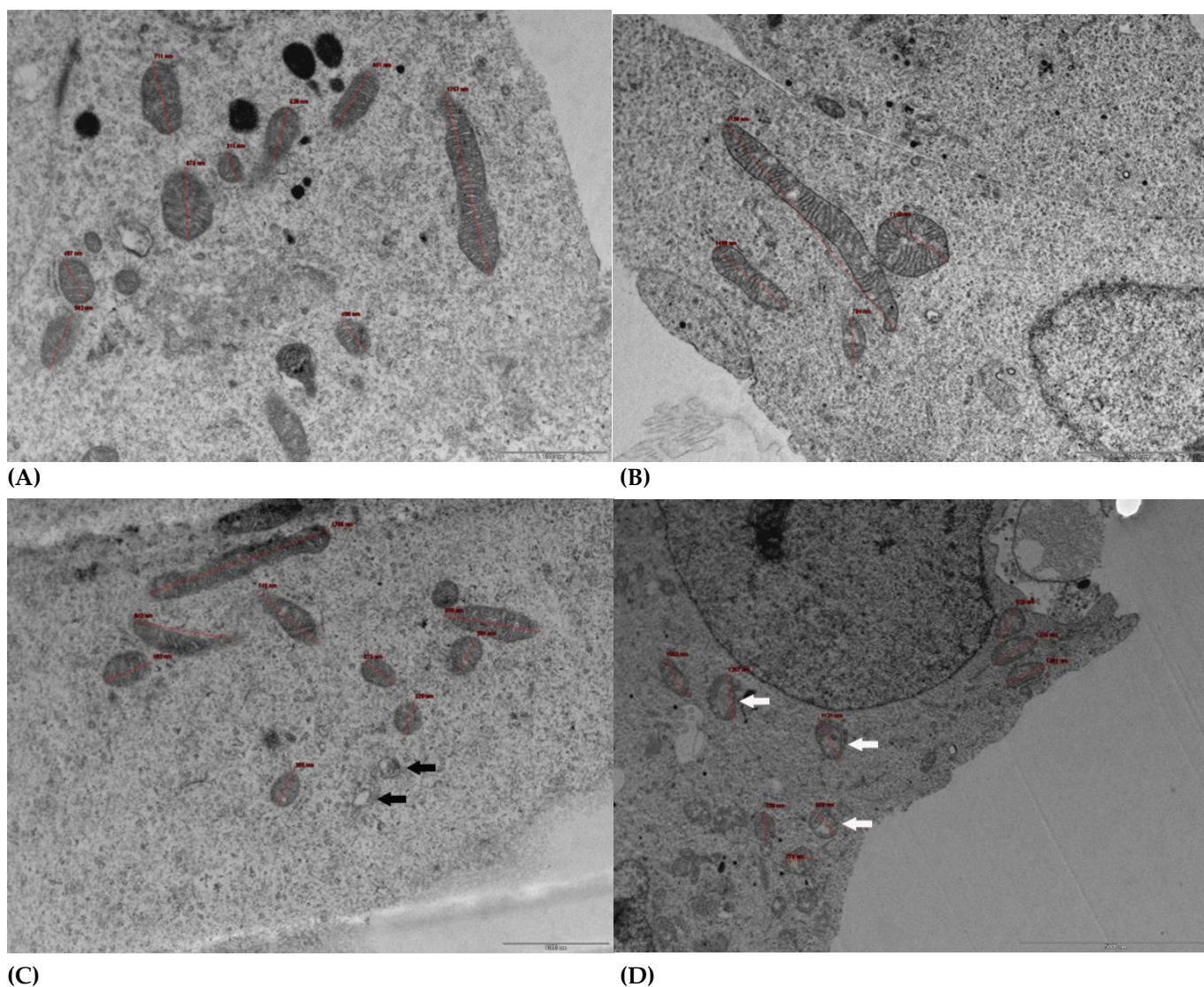


Figure 4: TEM images of control and alcohol treated cells.

(A) $\times 16500$ magnification of control (untreated) cells. Mitochondria are clear with well-visible cristae, some of which have been sized for reference. Scale bar: 1000 nm.

(B) $\times 9900$ magnification of cells treated with 50 mM ethanol for 24 hours. Mitochondria are distinguishable with visible cristae that are patchy in places, and some elongated mitochondria were observed. Mitochondrion measurements have been included for reference. Scale bar: 2000 nm.

(C) $\times 16500$ magnification of cells treated with 100 mM ethanol for 24 hours. Mitochondria are distinguishable with visible cristae that are patchy in places, some elongated mitochondria visible, and some vacuolar regions perhaps generated from mitophagy (examples indicated with black arrows). Mitochondrion measurements have been included for reference. Scale bar: 1000 nm.

(D) $\times 6000$ magnification of cells treated with 200 mM ethanol for 24 hours. Mitochondria are distinguishable with some visible cristae but clear regions within mitochondria (examples indicated with white arrows), and some vacuolar regions presumed to be generated from mitophagy. Mitochondrion measurements have been included for reference. Scale bar: 5000 nm.

For TEM transverse section images, up to 19 fields of view were analysed, with random unbiased selection. Images were captured using a MegaView SIS camera, with representative images included.

379
380

381
382
383

384

385
386

387
388
389

390
391
392
393

394
395
396
397

398
399

400
401

The effect of alcohol on cellular bioenergetic capacity was determined by quantitation of ATP levels. An alcohol-induced decline in ATP levels was observed which correlated with alcohol concentration and exposure duration and mirrored the MTT alcohol response curves for both undifferentiated and differentiated SH-SY5Y cells (Figures 5A–D, and Supplementary Table S6) and with similar IC_{50} values (refer to Table 1 and Supplementary Table S2). A significant reduction of ATP levels was evident from an exposure concentration of ≥ 20 mM and a 3-hour exposure for undifferentiated cells ($p < 0.0001$). Interestingly, the induction of cell metabolic activity (MTT assay results) observed after a 10 mM alcohol exposure was reiterated for ATP production. The resistance of differentiated cells to alcohol was also evident from measurements of ATP levels such that a significant reduction of ATP was from alcohol concentrations of ≥ 50 mM and for an application of at least 6 hours ($p = 0.0294$).

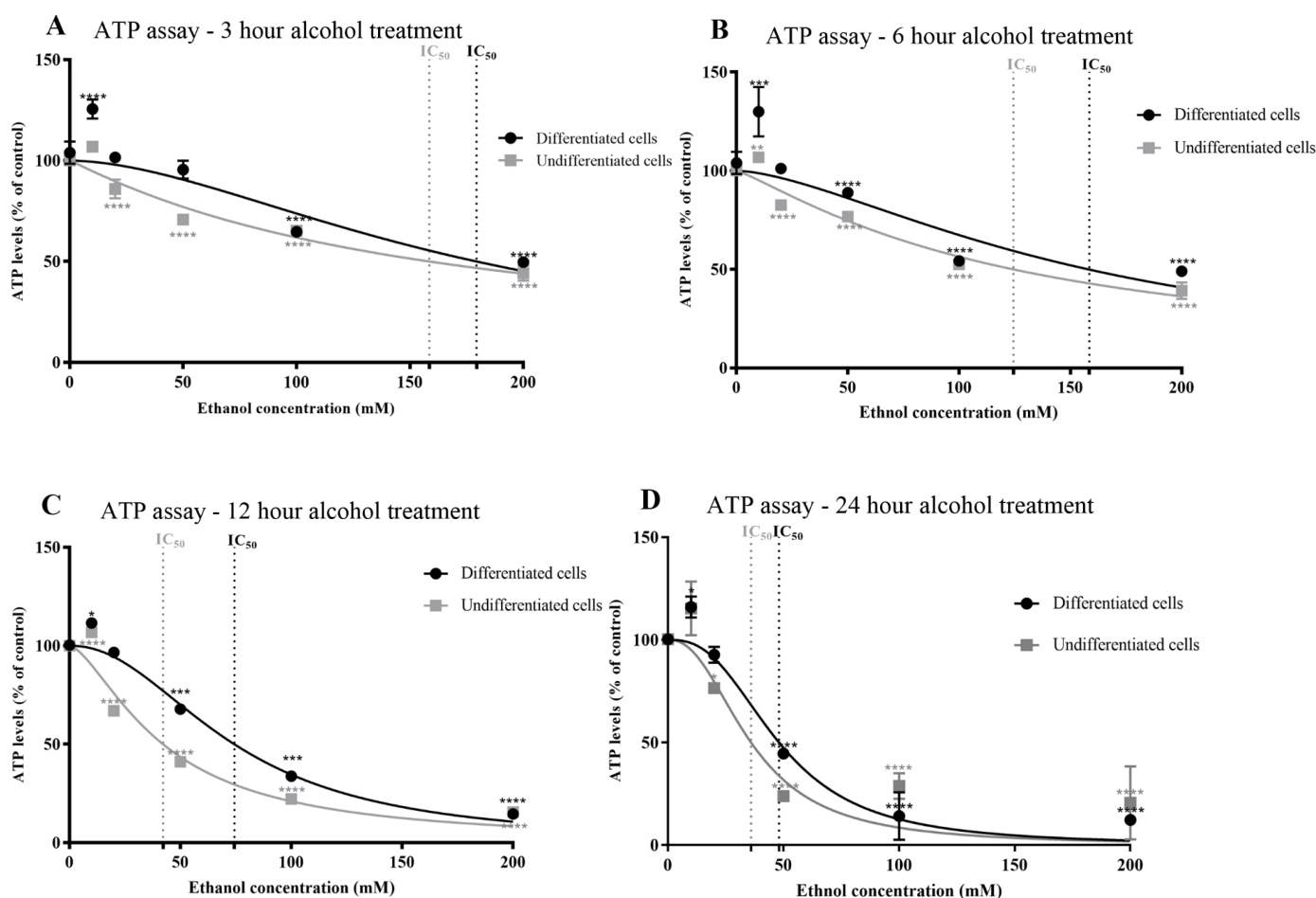


Figure 5: Alcohol effects on cellular ATP levels determined using an ATP bioluminescence assay.

Undifferentiated or differentiated SH-SY5Y cells were exposed to alcohol (0–200 mM) for durations of 3 (A), 6 (B), 12 (C), and 24 (D) hours, and the level of cellular ATP quantified using an ATP bioluminescence assay. Each data point represents a mean of at least 5 individual experiments. For marked significance: ** = p -value < 0.01 , *** = p -value < 0.001 , **** = p -value < 0.0001 .

The production of reactive oxygen species (ROS) was followed over the 3–24 hour time course by measuring the oxidation of 2',7'-dichlorodihydrofluorescein in a DCFDA assay. ROS levels increased in proportion to alcohol concentrations at all time points, with ROS levels that peaked at 3 and 6 hours (Figures 6A-D and Supplementary Table S7). Differentiated cells were notably more potent producers of ROS than undifferentiated cells, with significantly higher levels of ROS liberated after 20 and 50 mM alcohol exposures at the 3- and 6-hour time points ($p < 0.0001$) (Figures 6A-D and Supplementary Table S3).

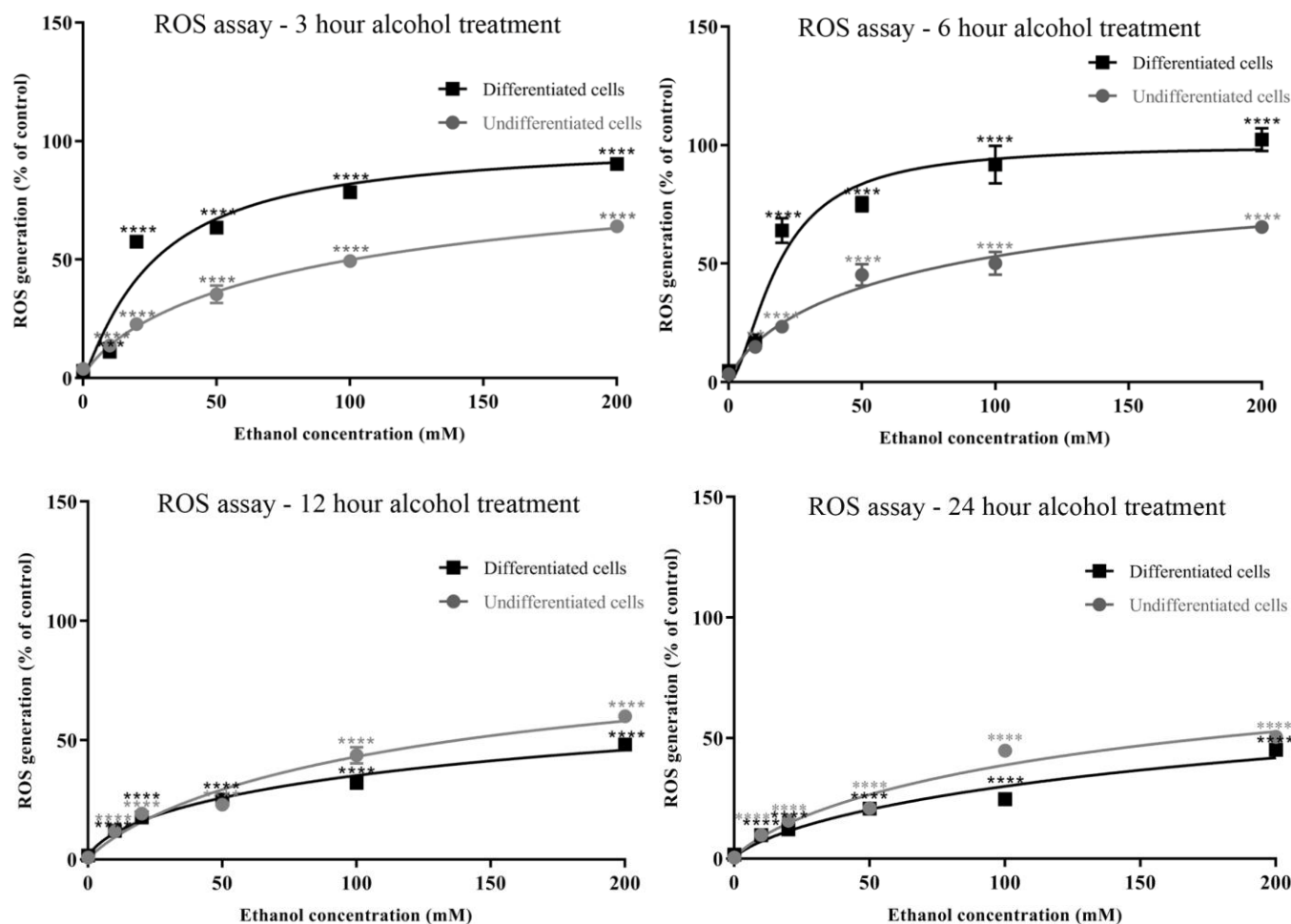


Figure 6: Alcohol induction of ROS levels determined using a DCFDA assay.

Undifferentiated or differentiated SH-SY5Y cells were exposed to alcohol (0–200 mM) for durations of 3 (A), 6 (B), 12 (C), and 24 (D) hours, and the levels of cellular ROS were quantified relative to that induced by H₂O₂. Each data point represents a mean of at least 5 individual experiments. For marked significance: ** = p-value < 0.01, *** = p-value < 0.001, **** = p-value < 0.0001.

In line with the production of cellular ROS, the level and time course of production of oxidatively-damaged proteins was quantified by determination of total protein carbonyl content (PCC). PCC increased in undifferentiated and differentiated SH-SY5Y cells in accordance with the concentration of alcohol; with significant levels detected from 10 mM alcohol, the lowest concentration examined ($p < 0.0001$) (Figures 7A,B). However, there was a delay in the accumulation of PCC, with significant increases above baseline (≈ 1 nmol/mg of protein) detected after 12 or 24 hours, and this had a higher positive correlation with ROS levels (Supplementary Table S8). PCC profiles were similar for undifferentiated cells and differentiated cells but with statistically higher levels in differentiated cells

from a threshold concentration of 50 mM and a 12-hour alcohol exposure ($p < 0.0001$) (Supplementary Table S3).

458
459

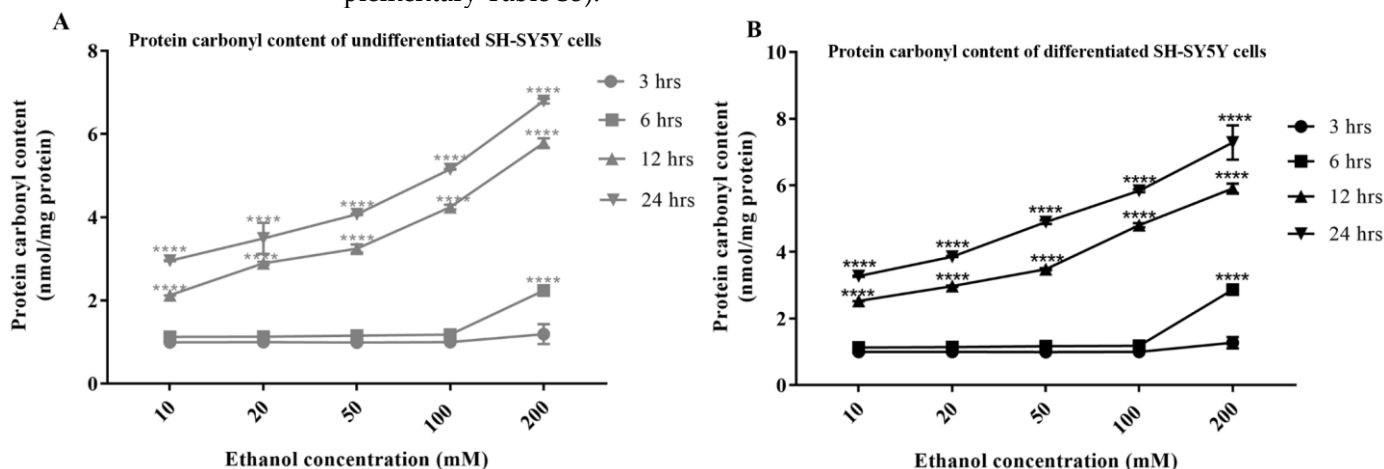


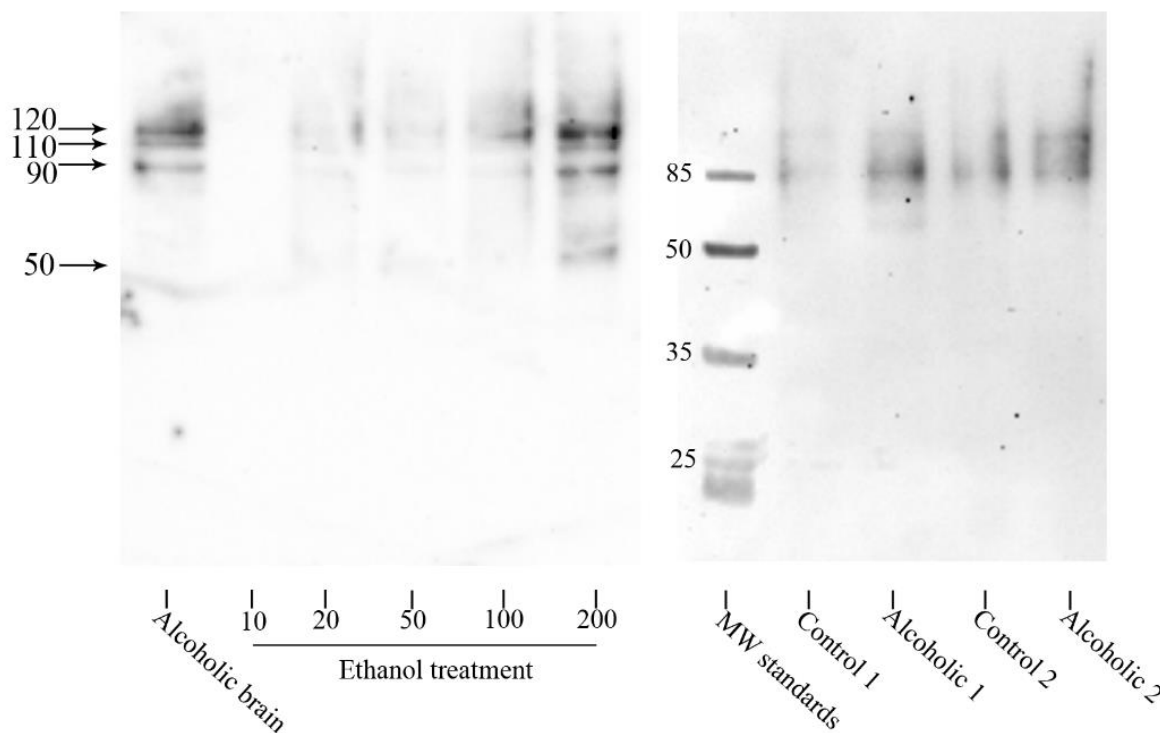
Figure 7: Alcohol induction of protein carbonyl content. Undifferentiated (A) or differentiated SH-SY5Y cells (B) were exposed to alcohol (0–200 mM) for durations of 3, 6, 12, and 24 hours, and the levels of protein carbonyl content (PCC) were quantified by spectrophotometry. Each data point represents the mean of at least 5 individual experiments. For marked significance: **** = p -value < 0.0001 .

460
461
462
463
464

In order to characterize the carbonylated proteins, an oxy-blot was performed. Carbonylation (protein oxidation) was detected in several proteins, at denatured molecular weights of 120, 110, 90, and 50 kDa, and with levels that increased in accordance with alcohol concentration (Figure 8). The profile of carbonylated proteins was similar to that detected in the brains of alcoholic subjects and to a lesser extent aged and sex-matched controls (Figure 8). Total PCC was increased in alcoholic brains compared to those of control subjects, with levels of approximately 4–8 nmols/mg of protein in the alcoholic brain samples, similar to those detected after the highest acute alcohol treatment to cells (Figure 8).

465
466
467
468
469
470
471
472
473

Carbonylated proteins



474

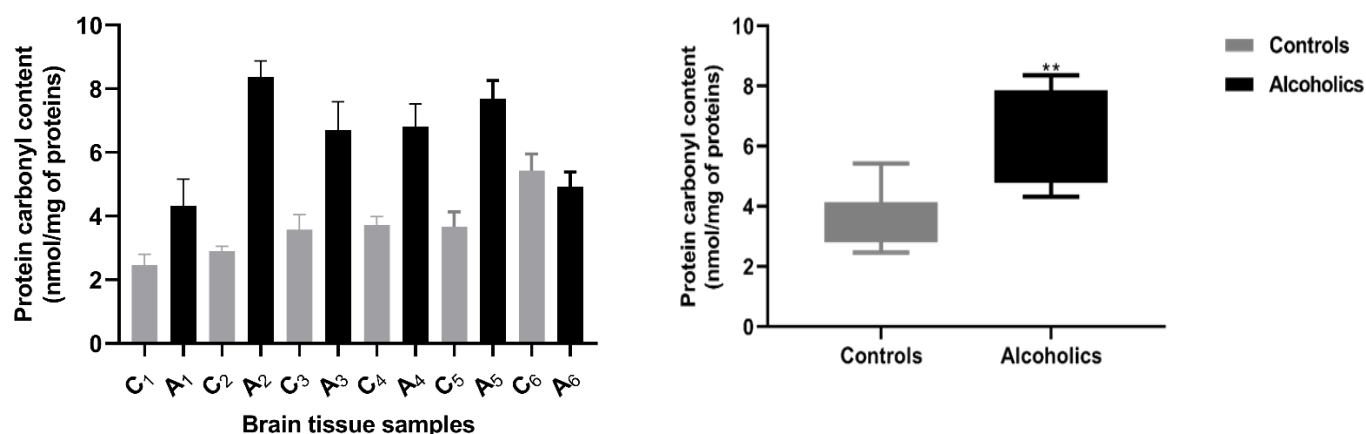


Figure 8: Quantitation and characterization of carbonylated proteins.

Differentiated SH-SY5Y cells were exposed to alcohol (10–200 mM) for 24 hours and carbonylated proteins were detected by an oxyblot. Major carbonylated proteins were detected at 120, 110, 90, and 50 kDa in cells and control or alcoholic brain tissue (upper panel). Protein carbonylated content of proteins from six control and six matched alcoholic brain tissue samples were quantified by spectrophotometry (lower panels). Each data point or blotting image is a representation of at least 3 individual experiments. For significance: ** = p-value < 0.01.

4. Discussion

Alcohol has toxic effects on the brain that may be particularly detrimental during periods of neurogenesis and differentiation, such as that experienced during neurodevelopment. To consider this further, and the potential involvement of redox stress, a comparison of alcohol neurotoxicity was undertaken between undifferentiated neuroblastoma cells and those that had been acutely differentiated into a neuronal phenotype. Cytotoxicity assessment using MTT and LDH assays showed that differentiation rendered cells more resistant to alcohol with higher alcohol concentrations required to reduce cell viability. However, somewhat contrary to alcohol's effects on cell viability, the levels of ROS and corresponding production of carbonylated (oxidatively-damaged) proteins were more extensive in differentiated cells. The characterization of carbonylated proteins revealed proteins with denatured molecular weights that overlapped with those present within the brains of alcoholic subjects, and further, PCC increased in alcoholics compared to matched controls. Hence, cell differentiation may promote resistance to alcohol-induced death but render cells more susceptible to the accumulation of oxidatively-damaged proteins.

We chose to model alcohol neurotoxicity using SH-SY5Y cells due to their human origin, broad application for neurotoxicity studies and potential for manipulation to cell cycle synchronized, trophic-dependent, differentiated cells that display morphology, neuritic arborization and protein expression indicative of neurons [46,47,56–59] (Supplementary Figure S1). We assessed the cytotoxicity of alcohol using MTT and LDH assays, as well as through visual inspection of cells to confirm reduced viability (Figures 1–3, and Supplementary Figures S1). Cell viability using MTT assays primarily relies on the activity of oxidoreductase and dehydrogenase enzymes in healthy (metabolically active) cells [60]. However, relatively low concentrations of agents, such as phytochemicals, can induce cell metabolic activity, with optical density readings that exceed those of control values [52], and this was observed after incubations with 10 mM alcohol (Figure 1). We, therefore, undertook another independent method for the quantification of changes in cell viability, using the liberation of extracellular LDH, due to a loss of membrane integrity

[61]. Both methods generated similar IC_{50} values for undifferentiated or differentiated cells to those from MTT assays. Surprisingly, IC_{50} values were higher for differentiated cells (Table 1); indicative that differentiation was protective against alcohol. This contrasts with the effects of some toxic agents, such as organophosphate and carbamate pesticides which are more toxic to differentiated SH-SY5Y cells [46], but not to other neurotoxicants, such as 1-methyl-4-phenyl-1,2,3,6-tetrahydropyridine (MPTP) [62], an agent that can induce Parkinsonian phenotypes in animals [63,64].

Cell viability experiments were undertaken across a broad concentration range of 10–200 mM alcohol and for 3–24 hours. This starting point for cell toxicity assays reflected the blood alcohol concentrations (BACs) of 0.04–0.05% (\approx 9–11 mM) that represent a central nervous system (CNS) threshold for impact on psychomotor tasks [65]. The exposures of 20 to 50 mM alcohol correspond to BACs that can arise from the consumption of several alcoholic beverages in a period of a few hours, concentrations consistent with intoxication for susceptible individuals [65]. The very high concentrations of 100 and 200 mM alcohol that were assessed can induce a loss of consciousness, coma, or even death, although patients with alcohol use disorders (AUDs) often develop tolerance to alcohol's CNS effects as well as display heightened alcohol metabolism enabling them to withstand such high systemic BACs (>100 mM), and still may not display signs of intoxication [66].

Alcohol can damage and alter the morphology of mitochondria, and promote the liberation of ROS [67,68]. We, therefore, investigated the ability of alcohol to affect cellular ATP levels and the production of ROS. The time course of ATP decline in response to alcohol mirrored the concentration-response curves observed from MTT and LDH assays, consistent with a shutdown of ATP production and loss of cell viability [69]. The opacity of the inner mitochondrial regions was reduced after exposure to the higher alcohol concentrations, with mitochondria observed as less electron-dense within the cristae (Figure 4), and this may correlate with a lowered ability to synthesize ATP [70]. Additionally, the capacity to produce ATP would be reduced if sufficient mitochondria are damaged to trigger mitophagy and their removal, and at higher concentrations of alcohol exposures, more vacuoles were evident which may have arisen from ongoing mitophagy (Figure 4).

Alcohol exposure induced ROS and increased the levels of oxidatively-damaged proteins. Relatively low levels of ROS can impact cellular signalling pathways and may be functional but there is a threshold at which ROS levels are detrimental to the cell and will induce apoptosis [71]. Our studies show that alcohol induced ROS production and increased protein carbonyl content at the lowest alcohol exposures examined (10 mM) (Figure 6) and for these exposures, there was no reduction in cell viability (Figures 1 and 2). By contrast, higher alcohol concentrations (and exposure durations) increased ROS production and reduced cell viability, in keeping with the ability of alcohol to induce apoptotic cell death [40–43]. From alcohol exposures of 20 mM, immuno-blotting provided a means to characterize the major proteins that were oxidatively-damaged and it was noteworthy that the proteins that accumulated oxidative damage after exposure to alcohol in vitro mirrored those observed in brain tissue from control and alcoholic patients. This suggests that there is a subset of cellular proteins that are particularly vulnerable to oxidative damage.

The endogenous levels of oxidative damage in alcoholic brains were similar to those from the highest induction of cellular toxicity in vitro (100–200 mM alcohol exposures) and were higher than those from age and sex-matched control subjects (Figures 8A, B). The molecular weights of these proteins (120, 100, 90, and 50 kDa) are similar to those that accumulated in SH-SY5Y cells in response to exposures to organophosphate and carbamate pesticides [46] and this presumably reflects their relative abundance and vulnerability to oxidation. We have postulated that these protein bands may include MAP-tau and tubulin (90 and 50 kDa, respectively) due to their increased expression during differentiation [46], but the identity of these proteins, and how oxidative damage could influence protein function, will need to be addressed in future studies.

5. Conclusions

Our results show that newly differentiated neuronal cells are, surprisingly, more resistant to cell death from alcohol than undifferentiated cells. However, for similar alcohol exposures, alcohol induced higher levels of ROS and the formation of oxidatively-damaged proteins in newly differentiated cells. Neuritic arborization was blunted and neuronal cells were killed after 6- and 12-hour exposures of ≥ 50 mM alcohol; levels of alcohol that would correspond to exposures only likely to be experienced by sustained excessive drinking, and not least, our experiments are limited since we cannot take account of reduced alcohol concentrations due to its metabolism. Our in vitro study is also limited in its capacity to reproduce the complexity of the multiple interacting cell types in vivo since only a single population of neuronal cells was examined. Furthermore, brain tissue exhibits regional damage to alcohol [29, 31–33] which may reflect differences in vulnerability between cell types, and our model may not be representative of other cell types. Nevertheless, a benefit of our approach is that the cells employed are homogenous, facilitating the generation of controlled experiments and reproducible and robust experimental data.

Since the lowest concentrations of alcohol examined (10 mM) can still induce the production of ROS and increase the levels of carbonylated proteins, depending on the turnover of these proteins, they could persist and impact neuronal cell function. Hence, the reduced cognitive capacity that arises in FASD [38–40] or that experienced by chronic heavy drinkers [9,11,14], could reflect both a reduction in neuronal number and the cellular damage and limited functional capacity of surviving neurons. This raises the possibility that countering the induction of oxidative stress, such as through enhancement of the cellular antioxidant capacity, could have benefits to acute and possibly chronic alcohol exposures by reducing the potential for neuronal loss and accrued oxidative damage.

Supplementary Materials: The following supporting information can be downloaded at: www.mdpi.com/xxx/s1, Supplementary Table S1: Demographics of the human brain samples. Supplementary Table S2: Alcohol toxicity to undifferentiated and differentiated SH-SY5Y cells measured by a MTT assay. Supplementary Table S3: A comparison of the effects of alcohol on undifferentiated vs differentiated SHSY-5Y cells. Supplementary Table S4: Alcohol toxicity to undifferentiated and differentiated SH-SY5Y cells measured by a LDH assay. Supplementary Table S5: Neurite reduction in response to alcohol treatment. Supplementary Table S6: Alcohol toxicity to undifferentiated and differentiated SH-SY5Y cells measured by a LDH assay. Supplementary Table S7: Alcohol induction of ROS in undifferentiated and differentiated SH-SY5Y cells measured by a DCFDA assay. Supplementary Table S8: Correlation between the levels of ROS and protein carbonyl content in response to alcohol exposures. Supplementary Figure S1: Treatment of undifferentiated and differentiated SHSY-5Y cells with alcohol. Figure S2: Samples of original Western oxy-blots.

Author Contributions: Conceptualization, A.W.M, W.G.C.; methodology, A.W.M, B.C.W., A.K., R.T., D.M.; validation, A.W.M, B.C.W., W.G.C.; formal analysis, A.W.M, B.C.W., A.K., W.G.C.; investigation, A.W.M, B.C.W., A.K., R.T., D.M., W.G.C.; resources, B.M., L.F.C., W.G.C.; writing—original draft preparation, A.W.M, W.G.C.; writing—review and editing, A.W.M, B.C.W., A.K., R.T., B.M., L.F.C., W.G.C.; supervision, W.G.C.; project administration, W.G.C.; funding acquisition, A.W.M, W.G.C, L.F.C. All authors have read and agreed to the published version of the manuscript.

Funding: This research was funded by a UK Foreign, Commonwealth and Development Office (FCDO) Commonwealth Scholarship Commission (UK) PhD award to AWM. This research was also supported by the European Foundation for Alcohol Research (ERAB) (EA 18 19 to LFC) and the Basque Government (grant number IT1512/22).

Institutional Review Board Statement: The human brain samples used in this study were used in accordance with the Human Tissue Act (2004) (UK) and were supplied by the Neuropsychopharmacology Re-search Group from the Department of Pharmacology of the University of the Basque Country (UPV/EHU). (<https://www.ehu.es/en/web/neuropsicofarmacologia/home>). Brain collection was conducted in compliance with policies of research and ethical review boards for post-mortem brain studies (Basque Institute of Legal Medicine, Bilbao, Spain) and is registered in the

National Biobank Register of the Spanish Health Department with the study number C.0000035 (https://biobancos.isciii.es/ListadoColecciones.aspx). 619
620

Data Availability Statement: Additional data that supports this work is available as Supplementary data files. 621
622

Acknowledgments: The authors would like to thank the staff members of the Basque Institute of Legal Medicine, Spain for their assistance with this study. 623
624

Conflicts of Interest: The authors declare no conflicts of interest. 625

References 626

1. Rehm, J.; Room, R.; Monteiro, M.; Gmel, G.; Graham, K.; Rehn, N.; Sempos, C. T.; Jernigan, D. Alcohol as a risk factor for global burden of disease. *Eur. Addict. Res.* 2003, 9, 157-164. 627
628
2. Rehm, J.; Mathers, C.; Popova, S.; Thavorncharoensap, M.; Teerawattananon, Y.; Patra, J. Global burden of disease and injury and economic cost attributable to alcohol use and alcohol-use disorders. *Lancet* 2009, 373, 2223-2233. 630
631
3. Global burden of disease (GBD) 2016 Alcohol Collaborators (2018) Alcohol use and burden for 195 countries and territories, 1990-2016: a systematic analysis for the Global Burden of Disease Study 2016. *Lancet* 2018, 392, 1015-1035. 632
633
4. Global status report on alcohol and health 2018. World Health Organization: Geneva, Switzerland, 2018. Available online: https://www.who.int/substance_abuse/publications/global_alcohol_report/en/ (accessed on the 31st of March 2024) 634
635
5. World Health Organization, 2022. Alcohol factsheet: <https://www.who.int/news-room/fact-sheets/detail/alcohol> (accessed on the 31st of March 2024). 636
637
6. Rehm, J.; Room, R.; Graham, K.; Monteiro, M.; Gmel, G.; Sempos, C. T. The relationship of average volume of alcohol consumption and patterns of drinking to burden of disease: an overview. *Addiction*, 2003, 98, 1209-1228. 638
639
7. Rehm, J.; Gmel, G. E.; Sr., Gmel, G.; Hasan, O. S. M.; Imtiaz, S.; Popova, S.; Probst, C.; Roerecke, M.; Room, R.; Samokhvalov, A. V. et al. The relationship between different dimensions of alcohol use and the burden of disease-an update. *Addiction* 2017, 112, 968-1001. 640
641
642
8. Rehm, J.; Taylor, B.; Mohapatra, S.; Irving, H.; Baliunas, D.; Patra, J. Roerecke, M. Alcohol as a risk factor for liver cirrhosis: a systematic review and meta-analysis. *Drug Alcohol Rev.* 2010, 29, 437-445. 643
644
9. Anstey, K. J.; Mack, H. A.; Cherbuin, N. Alcohol consumption as a risk factor for dementia and cognitive decline: meta-analysis of prospective studies. *Am. J. Geriatr. Psychiatry* 2009, 17, 542-555. 645
646
10. Ronksley, P. E.; Brien, S. E.; Turner, B. J.; Mukamal, K. J.; Ghali, W. A. Association of alcohol consumption with selected cardiovascular disease outcomes: a systematic review and meta-analysis. *B.M.J.* 2011, 342, d671. 647
648
11. Sabia, S.; Elbaz, A.; Britton, A.; Bell, S.; Dugravot, A.; Shipley, M.; Kivimaki, M.; Singh-Manoux, A. Alcohol consumption and cognitive decline in early old age, *Neurology* 2014, 82, 332-339. 649
650
12. Holst, C.; Tolstrup, J. S.; Sorensen, H. J.; Becker, U. Alcohol dependence and risk of somatic diseases and mortality: a cohort study in 19 002 men and women attending alcohol treatment. *Addiction* 2017, 112, 1358-1366. 651
652
13. Xu, W. ; Wang, H. ; Wan, Y. ; Tan, C. ; Li, J. ; Tan, L. ; Yu, J. T. Alcohol consumption and dementia risk: a dose-response meta-analysis of prospective studies. *Eur. J. Epidemiol.* 2017, 32, 31-42. 653
654
14. Topiwala, A.; Ebmeier, K. P. Effects of drinking on late-life brain and cognition. *Evid. Based Ment. Health* 2018, 21, 12-15. 655
15. Schwarzwinger, M.; Pollock, B. G.; Hasan, O. S. M.; Dufouil, C.; Rehm, J.; QalyDays Study Group. Contribution of alcohol use disorders to the burden of dementia in France 2008-13: a nationwide retrospective cohort study. *Lancet Public Health* 2018, 3, e124-e132. 656
657
658
16. Wang G, Li DY, Vance DE, Li W. Alcohol Use Disorder as a Risk Factor for Cognitive Impairment. *J Alzheimers Dis.* 2023;94(3):899-907. 659
660
17. Kilian C, Klinger S, Rehm J, Manthey J. Alcohol use, dementia risk, and sex: a systematic review and assessment of alcohol-attributable dementia cases in Europe. *BMC Geriatr.* 2023 Apr 25;23(1):246. 661
662
18. Jensen, G. B.; Pakkenberg, B. Do alcoholics drink their neurons away? *Lancet* 1993, 342, 1201-1204. 663
19. Harper, C. The neuropathology of alcohol-specific brain damage, or does alcohol damage the brain? *J. Neuropathol. Exp. Neurol.* 1998, 57, 101-110. 664
665
20. Kril, J. J.; Halliday, G. M. Brain shrinkage in alcoholics: A decade on and what have we learned? *Prog. Neurobiol.* 1999, 58, 381-387. 666
667
21. Zahr, N. M.; Kaufman, K. L.; Harper, C. G. Clinical and pathological features of alcohol-related brain damage. *Nat. Rev. Neurol.* 2011, 7, 284-294. 668
669
22. Skuja, S.; Groma, V.; Smane, L. Alcoholism and cellular vulnerability in different brain regions. *Ultrastruct. Pathol.* 2012, 36, 40-47. 670
671
23. Whittom, A.; Villarreal, A.; Soni, M.; Owusu-Duku, B.; Meshram, A.; Rajkowska, G.; Stockmeier, C. A.; Miguel-Hidalgo, J. J. Markers of apoptosis induction and proliferation in the orbitofrontal cortex in alcohol dependence. *Alcohol Clin. Exp. Res.* 2014, 38, 2790-2799. 672
673
674

24. Erdozain, A. M.; Morentin, B.; Bedford, L.; King, E.; Tooth, D.; Brewer, C.; Wayne, D.; Johnson, L.; Gerdes, H. K.; Wigmore, P. et al. Alcohol-related brain damage in humans. *PLoS One* 2014, 9(4), e93586. 675
676
25. Labisso, W. L.; Raulin, A. C.; Nwidu, L. L.; Kocon, A.; Wayne, D.; Erdozain, A. M.; Morentin, B.; Schwendener, D.; Allen, G.; Enticott, J.; et al. The loss of alpha- and beta-tubulin proteins are a pathological hallmark of chronic alcohol consumption and natural brain ageing. *Brain Sci.* 2018, 8(9). 677
678
679
26. Monnig, M. A.; Tonigan, J. S.; Yeo, R. A.; Thoma, R. J.; McCrady, B. S. White matter volume in alcohol use disorders: a meta-analysis. *Addict. Biol.* 2013, 18, 581-592. 680
681
27. Xiao, P.; Dai, Z.; Zhong, J.; Zhu, Y.; Shi, H.; Pan, P. Regional gray matter deficits in alcohol dependence: A meta-analysis of voxel-based morphometry studies. *Drug Alcohol Depend.* 2015, 153, 22-28. 682
683
28. Yang, X.; Tian, F.; Zhang, H.; Zeng, J.; Chen, T.; Wang, S.; Jia, Z.; Gong, Q. Cortical and subcortical gray matter shrinkage in alcohol-use disorders: a voxel-based meta-analysis. *Neurosci. Biobehav. Rev.* 2016, 66, 92-103. 684
685
29. Zahr, N. M.; Pfefferbaum, A. Alcohol's effects on the brain: neuroimaging results in humans and animal models. *Alc. Res.* 2017, 38, 183-206. 686
687
30. Topiwala, A.; Allan, C. L.; Valkanova, V.; Zsoldos, E.; Filippini, N.; Sexton, C.; Mahmood, A.; Fooks, P.; Singh-Manoux, A.; Mackay, C. E. et al. Moderate alcohol consumption as risk factor for adverse brain outcomes and cognitive decline: longitudinal cohort study. *B.M.J.* 2017, 357, j2353. 688
689
690
31. Fritz, M.; Klawonn, A. M.; Zahr, N. M. Neuroimaging in alcohol use disorder: From mouse to man. *J. Neurosci. Res.* 2019, 1-19. 691
692
32. Shim, J. H.; Kim, Y. T.; Kim, S.; Baek, H. M. Volumetric reductions of subcortical structures and their localizations in alcohol-dependent patients. *Front. Neurol.* 2019, 10, 247. 693
694
33. Daviet R, Aydogan G, Jagannathan K, Spilka N, Koellinger PD, Kranzler HR, Nave G, Wetherill RR. Associations between alcohol consumption and gray and white matter volumes in the UK Biobank. *Nat Commun.* 2022 Mar 4;13(1):1175. 695
696
34. Immonen, S., Launes, J., Järvinen, I. et al. Moderate alcohol use is associated with decreased brain volume in early middle age in both sexes. *Sci Rep* 10, 13998 (2020). <https://doi.org/10.1038/s41598-020-70910-5> 697
698
35. Lees B, Meredith LR, Kirkland AE, Bryant BE, Squeglia LM. Effect of alcohol use on the adolescent brain and behavior. *Pharmacol Biochem Behav.* 2020 May;192:172906. doi: 10.1016/j.pbb.2020.172906 699
700
36. Squeglia LM, Boissoneault J, Van Skike CE, Nixon SJ, Matthews DB. Age-related effects of alcohol from adolescent, adult, and aged populations using human and animal models. *Alcohol Clin Exp Res.* 2014 Oct;38(10):2509-16. doi: 10.1111/acer.12531. 701
702
703
37. May PA, Blankenship J, Marais AS, Gossage JP, Kalberg WO, Joubert B, Cloete M, Barnard R, De Vries M, Hasken J, Robinson LK, Adnams CM, Buckley D, Manning M, Parry CD, Hoyme HE, Tabachnick B, Seedat S (2013) Maternal alcohol consumption producing fetal alcohol spectrum disorders (FASD): quantity, frequency, and timing of drinking. *Drug Alcohol Depend* 133:502–512 704
705
706
707
38. Flak AL, Su S, Bertrand J, Denny CH, Kesmodel US, Cogswell ME (2014) The association of mild, moderate, and binge prenatal alcohol exposure and child neuropsychological outcomes: a meta-analysis. *Alcohol Clin Exp Res* 38:214–226 708
709
39. Wilhelm, C. J., & Guizzetti, M. (2016). Fetal Alcohol Spectrum Disorders: An Overview from the Glia Perspective. *Frontiers in Integrative Neuroscience*, 9, 170319. <https://doi.org/10.3389/fmint.2015.00065> 710
711
40. Popova, S., Charness, M.E., Burd, L. et al. Fetal alcohol spectrum disorders. *Nat Rev Dis Primers* 9, 11 (2023). <https://doi.org/10.1038/s41572-023-00420-x> 712
713
41. Haorah J, Ramirez SH, Floreani N, Gorantla S, Morsey B, Persidsky Y. Mechanism of alcohol-induced oxidative stress and neuronal injury. *Free Radic Biol Med.* 2008 Dec 1;45(11):1542-50. doi: 10.1016/j.freeradbiomed.2008.08.030. 714
715
42. Birková A, Hubková B, Čížmárová B, Bolerázská B. Current View on the Mechanisms of Alcohol-Mediated Toxicity. *Int J Mol Sci.* 2021 Sep 7;22(18):9686. doi: 10.3390/ijms22189686 716
717
43. Tsermpini EE, Plemenitaš Ilješ A, Dolžan V. Alcohol-Induced Oxidative Stress and the Role of Antioxidants in Alcohol Use Disorder: A Systematic Review. *Antioxidants (Basel).* 2022 Jul 15;11(7):1374. doi: 10.3390/antiox11071374. 718
719
44. Gimenez-Gomez P, Le T, Martin GE. Modulation of neuronal excitability by binge alcohol drinking. *Front Mol Neurosci.* 2023 Feb 14;16:1098211. doi: 10.3389/fnmol.2023.1098211. 720
721
45. Granato A, Dering B. Alcohol and the Developing Brain: Why Neurons Die and How Survivors Change. *Int J Mol Sci.* 2018 Sep 30;19(10):2992. doi: 10.3390/ijms19102992 722
723
46. Mudyanselage AW, Wijamunige BC, Kocon A, Carter WG. Differentiated Neurons Are More Vulnerable to Organophosphate and Carbamate Neurotoxicity than Undifferentiated Neurons Due to the Induction of Redox Stress and Accumulate Oxidatively-Damaged Proteins. *Brain Sci.* 2023 Apr 26;13(5):728. doi: 10.3390/brainsci13050728. 724
725
726
47. Shipley, M.M.; Mangold, C.A.; Szpara, M.L. Differentiation of the SH-SY5Y human neuroblastoma cell line. *J. Vis. Exp.* 2016, 108, 53193. 727
728
48. Raghunath M, Patti R, Bannerman P, Lee CM, Baker S, Sutton LN, Phillips PC, Damodar Reddy C. A novel kinase, AATYK induces and promotes neuronal differentiation in a human neuroblastoma (SH-SY5Y) cell line. *Brain Res Mol Brain Res.* 2000 May 5;77(2):151-62. doi: 10.1016/s0169-328x(00)00048-6. 729
730
731
49. Pool M, Thiemann J, Bar-Or A, Fournier AE. NeuriteTracer: a novel ImageJ plugin for automated quantification of neurite outgrowth. *J Neurosci Methods.* 2008 Feb 15;168(1):134-9. doi: 10.1016/j.jneumeth.2007.08.029. 732
733

50. Elmorsy E, Attalla S, Fikry E, et al. Adverse effects of anti-tuberculosis drugs on HepG2 cell bioenergetics. *Human & Experimental Toxicology*. 2017;36(6):616-625. doi:10.1177/0960327116660751 734
51. Elmorsy, E.; Al-Ghafari, A.; Almutairi, F. M.; Aggour, A. M.; Carter, W. G. Antidepressants are cytotoxic to rat primary blood brain barrier endothelial cells at high therapeutic concentrations. *Toxicol. In Vitro* 2017, 44, 154-163. 735
52. ALNasser MN, AlSaadi AM, Whitby A, Kim DH, Mellor IR, Carter WG. Acai Berry (*Euterpe* sp.) Extracts Are Neuroprotective against L-Glutamate-Induced Toxicity by Limiting Mitochondrial Dysfunction and Cellular Redox Stress. *Life (Basel)*. 2023 Apr 15;13(4):1019. doi: 10.3390/life13041019. 736
53. El Sharazly, B.M.; Ahmed, A.; Elsheikha, H.M.; Carter, W.G. An In Silico and In Vitro Assessment of the Neurotoxicity of Mefloquine. *Biomedicines* 2024, 12, 505. <https://doi.org/10.3390/biomedicines12030505>. 737
54. Lowry, O. H.; Rosebrough, N. J.; Farr, A. L.; Randall, R. J. Protein measurement with the Folin phenol reagent. *J. Biol. Chem.* 1951, 193, 265-275. 738
55. Vigneswara, V.; Lowenson, J. D.; Powell, C. D.; Thakur, M.; Bailey, K.; Clarke, S.; Ray, D. E.; Carter, W. G. Proteomic identification of novel substrates of a protein isoaspartyl methyltransferase repair enzyme. *J. Biol. Chem.* 2006, 281, 32619-32629. 739
56. Encinas, M.; Iglesias, M.; Liu, Y.; Wang, H.; Muhaisen, A.; Ceña, V.; Gallego, C.; Comella, J.X. Sequential Treatment of SH-SY5Y Cells with Retinoic Acid and Brain-Derived Neurotrophic Factor Gives Rise to Fully Differentiated, Neurotrophic Factor Dependent, Human Neuron-Like Cells. *J. Neurochem.* 2000, 75, 991-1003. 740
57. Cheung, Y.-T.; Lau, W.K.-W.; Yu, M.-S.; Lai, C.S.-W.; Yeung, S.-C.; So, K.-F.; Chang, R.C.-C. Effects of all-trans-retinoic acid on human SH-SY5Y neuroblastoma as in vitro model in neurotoxicity research. *NeuroToxicology* 2009, 30, 127-135. 741
58. Lopez-Suarez, L.; Awabdh, S.A.; Coumoul, X.; Chauvet, C. The SH-SY5Y human neuroblastoma cell line, a relevant in vitro cell model for investigating neurotoxicology in human: Focus on organic pollutants. *Neurotoxicology* 2022, 92, 131-155. 742
59. Kovalevich, J.; Langford, D. Considerations for the use of SH-SY5Y neuroblastoma cells in neurobiology. *Methods Mol. Biol.* 2013, 1078, 9-21. 743
60. Ghasemi M, Turnbull T, Sebastian S, Kempson I. The MTT Assay: Utility, Limitations, Pitfalls, and Interpretation in Bulk and Single-Cell Analysis. *Int J Mol Sci.* 2021 Nov 26;22(23):12827. doi: 10.3390/ijms222312827. 744
61. Kaja, S.; Payne, A.J.; Naumchuk, Y.; Koulen, P. Quantification of Lactate Dehydrogenase for Cell Viability Testing Using Cell Lines and Primary Cultured Astrocytes. *Curr. Protoc. Toxicol.* 2017, 72, 2.26.1-2.26.10. 745
62. Elmorsy, E.; Al-Ghafari, A.; Al Doghaither, H.; Hashish, S.; Salama, M.; Mudyanselage, A.W.; James, L.; Carter, W.G. Differential Effects of Paraquat, Rotenone, and MPTP on Cellular Bioenergetics of Undifferentiated and Differentiated Human Neuroblastoma Cells. *Brain Sci.* 2023, 13, 1717. <https://doi.org/10.3390/brainsci13121717> 746
63. Thirugnanam T, Santhakumar K. Chemically induced models of Parkinson's disease. *Comp Biochem Physiol C Toxicol Pharmacol.* 2022 Feb;252:109213. doi: 10.1016/j.cbpc.2021.109213. 747
64. Prakash, S.; Carter, W.G. The Neuroprotective Effects of Cannabis-Derived Phytocannabinoids and Resveratrol in Parkinson's Disease: A Systematic Literature Review of Pre-Clinical Studies. *Brain Sci.* 2021, 11, 1573. 748
65. Eckardt, M. J.; File, S. E.; Gessa, G. L.; Grant, K. A.; Guerri, C.; Hoffman, P. L.; Kalant, H.; Koob, G. F.; Li, T. K.; Tabakoff, B. Effects of moderate alcohol consumption on the central nervous system. *Alcohol Clin. Exp. Res.* 1998, 22, 998-1040. 749
66. Urso, T.; Gavalier, B.S.; Van Thiel, T.H. Blood ethanol levels in sober alcohol users seen in an emergency room. *Life Sci.* 1981, 28, 1053-1056. 750
67. Manzo-Avalos S, Saavedra-Molina A. Cellular and mitochondrial effects of alcohol consumption. *Int J Environ Res Public Health.* 2010 Dec;7(12):4281-304. doi: 10.3390/ijerph7124281. 751
68. Shang P, Lindberg D, Starski P, Peyton L, Hong SI, Choi S, Choi DS. Chronic Alcohol Exposure Induces Aberrant Mitochondrial Morphology and Inhibits Respiratory Capacity in the Medial Prefrontal Cortex of Mice. *Front Neurosci.* 2020 Oct 22;14:561173. doi: 10.3389/fnins.2020.561173. 752
69. Kamiloglu, S.; Sari, G.; Ozdal, T.; Capanoglu, E. Guidelines for cell viability assays. *Food Front.* 2020, 1, 332-349 753
70. Heine KB, Parry HA, Hood WR. How does density of the inner mitochondrial membrane influence mitochondrial performance? *Am J Physiol Regul Integr Comp Physiol.* 2023 Feb 1;324(2):R242-R248. doi: 10.1152/ajpregu.00254.2022. 754
71. Redza-Dutordoir M, Averill-Bates DA. Activation of apoptosis signalling pathways by reactive oxygen species. *Biochim Biophys Acta.* 2016 Dec;1863(12):2977-2992. doi: 10.1016/j.bbamcr.2016.09.012. 755

Disclaimer/Publisher's Note: The statements, opinions and data contained in all publications are solely those of the individual author(s) and contributor(s) and not of MDPI and/or the editor(s). MDPI and/or the editor(s) disclaim responsibility for any injury to people or property resulting from any ideas, methods, instructions or products referred to in the content. 782